Reciprocating flow-based centrifugal microfluidics mixer

Zahra Noroozi,[1] Horacio Kido,[1,2] Miodrag Micic,[1,3] Hansheng Pan,[4] Christian Bartolome,[4] Marko Princevac,[4] Jim Zoval,[1,5] and Marc Madou[1]
[1]*Department of Mechanical and Aerospace Engineering, University of California, Irvine, 4200 Engineering Gateway, Irvine, California 92697-3975, USA*
[2]*RotaPrep, Inc., 2913 El Camino Real, #242, Tustin, California 92782, USA*
[3]*MP Biomedicals LLC, 3 Hutton Centre, Suite 100, Santa Ana, California 92707, USA*
[4]*Department of Mechanical Engineering, University of California, Riverside, 900 University Avenue, Riverside, California 92521, USA*
[5]*Department of Chemistry, Division of Mathematical Science, Saddleback College, 28000 Marguerite Parkway, Mission Viejo, California 92692, USA*

(Received 14 April 2009; accepted 12 June 2009; published online 14 July 2009)

Proper mixing of reagents is of paramount importance for an efficient chemical reaction. While on a large scale there are many good solutions for quantitative mixing of reagents, as of today, efficient and inexpensive fluid mixing in the nanoliter and microliter volume range is still a challenge. Complete, i.e., quantitative mixing is of special importance in any small-scale analytical application because the scarcity of analytes and the low volume of the reagents demand efficient utilization of all available reaction components. In this paper we demonstrate the design and fabrication of a novel centrifugal force-based unit for fast mixing of fluids in the nanoliter to microliter volume range. The device consists of a number of chambers (including two loading chambers, one pressure chamber, and one mixing chamber) that are connected through a network of microchannels, and is made by bonding a slab of polydimethylsiloxane (PDMS) to a glass slide. The PDMS slab was cast using a SU-8 master mold fabricated by a two-level photolithography process. This microfluidic mixer exploits centrifugal force and pneumatic pressure to reciprocate the flow of fluid samples in order to minimize the amount of sample and the time of mixing. The process of mixing was monitored by utilizing the planar laser induced fluorescence (PLIF) technique. A time series of high resolution images of the mixing chamber were analyzed for the spatial distribution of light intensities as the two fluids (suspension of red fluorescent particles and water) mixed. Histograms of the fluorescent emissions within the mixing chamber during different stages of the mixing process were created to quantify the level of mixing of the mixing fluids. The results suggest that quantitative mixing was achieved in less than 3 min. This device can be employed as a stand alone mixing unit or may be integrated into a disk-based microfluidic system where, in addition to mixing, several other sample preparation steps may be included. © *2009 American Institute of Physics.*
[DOI: 10.1063/1.3169508]

I. INTRODUCTION

In recent years there has been an explosion of interest in miniaturization of complex and fully functional fluidic systems by integrating several chemical and mechanical processes on a small chip. The fundamental technology behind such systems is microfluidics.[1] Microfluidics is now widely used in chemical[2–5] and biological applications[6–10] where portability, low sample consumption, and cost are of interest and where scaling down might improve such important characteristics as heat management, dead volume, and speed of the process.[11]

Fluidic mixing is a basic step for many analytical applications and becomes more challenging with miniaturization of the fluidic system since the Reynolds (Re) number in small chambers is in the range of smaller than 1 to 10.[12] This renders the influence of viscous forces more significant and in some cases flow can be completely dominated by those forces (i.e., creeping flow, $\mathrm{Re} \ll 1$). Even though considerable progress has been made toward the development of strategies for improving the mixing of fluids with low Reynolds numbers, research in micromixing still remains in the spotlight. The mixing of two fluids involves a combination of three different mass transfer processes, i.e., molecular diffusion, turbulent or eddy diffusion, and bulk or large-scale diffusion.[13] While in the large scale, molecular diffusion as governed by Darcy's equation is an insignificant contributing factor to mixing, in the case of small structures and flows with low Re numbers, this process is the dominant mode of mixing.[14] The biggest drawback of this mixing mode is that it is too slow for any practical applications in which complete fluid mixing within a reasonable time frame is needed.

Molecular diffusion, as described by Darcy's equation, is the movement of flow particles by Brownian motion from the more concentrated to the less concentrated spaces in a medium. In order to mix two different streams of fluids moving alongside in a narrow channel, particles need to "jump" from one imaginary streamline to another. The interdiffusion time between the two streams is proportional to the square of the distance,[15]

$$t \sim \frac{d^2}{D}, \tag{1}$$

where d is the diffusion distance and D is the diffusion coefficient. Based on purely molecular diffusion, $D \sim 10^{-6}$ (m^2/s), a very long channel may be needed in order for the flow at the end of the channel to become fully homogenized. The reason for this is that molecular diffusion is a very short-range process and even for a small channel (say 100 μm in diameter), the structure size dictates that the distance is still too long for diffusion-based mixing to be considered as an efficient process within the typical timescale and fluid velocities expected from such microfluidic systems.

Looking at Darcy's equation in a different way, the volume mixed at lapsed time t can be described as

$$V \sim A\sqrt{Dt}, \tag{2}$$

where A is the surface area of mixing fluid. Mixing in microfluidics can therefore be accelerated by reducing the fluid elements over which particles have to diffuse, either by stretching, splitting, and folding of a fluid flow, or by multilamination of fluid elements in the flow. An efficient alternative method of mixing at the microscale is to promote chaotic advective flow by inducing the streamlines to intersect each other using time modulation of the flow field.[16] A number of different methods for promoting molecular diffusion-based mixing have been investigated.[17] Depending on the mechanism of operation, these methods can be classified as either active or passive.[18] In active mixing an external energy input is utilized to introduce local chaotic advection in the flow while in the passive mixing surface texturing is used to induce local chaotic advection events.

Some of the methods that have been previously explored to induce chaotic advection in microsystems include electroosmotic mixing by periodically varying the electric field to mix two aqueous flows,[19] magnetic stirring by using a magnetic field to rotate one or more magnetic bars within the fluid medium,[20,21] time pulsing by pulsing the flow rate in one of the inlets,[22] ultrasonic mixing using a piezoelectrically driven diaphragm at ultrasonic frequencies,[23] bubble mixing by interaction of the fluid with bubbles of gas introduced into the channels,[24] and actuation mixing using gold/polypyrrole (PPy) flaps.[25]

Passive mixing, as discussed above, employs modifications of the channel geometry to minimize diffusion distances and thus the mixing time.[26,27] This is achieved either by dividing the flow into several narrow streams (fluid elements) followed by recombination of these streams or by generating a fluid motion perpendicular to the main flow to stretch and fold the flow as it moves along the channel. Examples of passive micromixers include lamination micromixers,[28,29] serpentine micromixers,[30,31] Tesla's micromixers,[32] split-and-recombine micromixers,[33–36] and T-micromixers.[37–40]

Each of the previously mentioned methods has its advantages and disadvantages and depending on the specific application, some are more suitable than others. On the one hand, active mixers generally yield more effective mixing in shorter times and distances. However they require external power and/or moving parts that are complicated to fabricate and are less reliable due to their susceptibility to potential system or process failure. In addition, some sensitive biological applications may not tolerate the presence of factors such as applied electric fields, excessive heat, or mechanical shear stress. On the other hand, some of the three-dimensional (3D) passive mixers require complicated multilayer photolithography and are difficult to integrate into chip-based microfluidic systems.

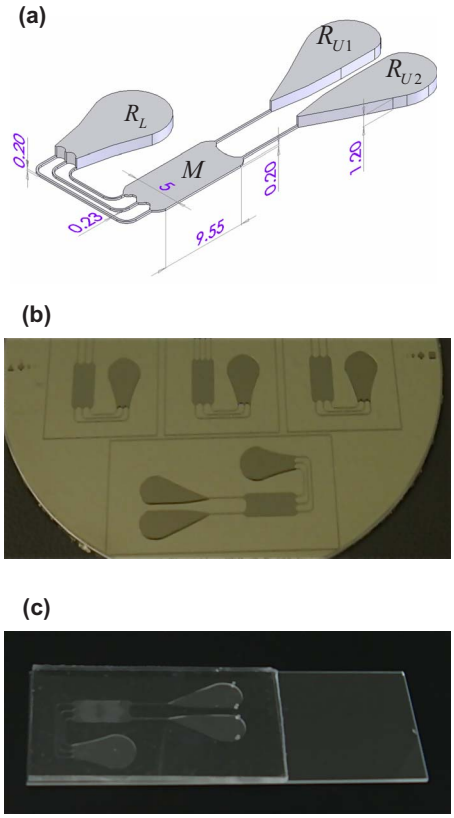

FIG. 1. (Color online) Microfluidics mixer cartridge. (a) Schematic illustration of micromixer unit; all units are in millimeters; (b) Photography of the of the SU-8 casting master mold; (c) Photography of the assembled PDMS/glass slide unit.

This work presents the design and fabrication of a centrifugal-based microfluidic unit for continuous mixing of small-scale (up to 30 μl) volumes of fluids in a disposable unit made from a polydimethylsiloxane (PDMS) slab and a glass slide as depicted in Fig. 1(c). The unit could be used as a stand-alone micromixer or it could be integrated onto a disk-based microfluidic integrated lab-on a disk system that may incorporate other functionalities, for example, sample lysis, separation of biomaterials, amplification of nucleic acids, detection of biomolecules, and other functions, as determined by the intended use and process flow of the device.

A two-level SU-8 master mold was fabricated using standard photolithographic methods to create shallow features including a mixing chamber and a network of channels, and deep features including two reservoirs for initial storage of the two fluids to be mixed, and another reservoir for storing pneumatic pressure. Centrifugal force[41] and the resulting pneumatic pressure accumulated in the system were utilized to propel the two fluids to be mixed into the mixing chamber

in a reciprocating manner [Fig. 1(a)]. In order to be able to follow and quantify the level of mixing, the fluid injected into the first reservoir consisted of an aqueous suspension of fluorescently labeled polystyrene particles in water, while the second fluid was water alone. The process of mixing was monitored using the planar laser induced fluorescence (PLIF) technique, which is a nonintrusive method for measuring scalar concentration in fluids. In this technique the level of local fluorescence emissions induced by laser excitation is proportional to particle/dye concentration. A time series of high resolution images of the mixing chamber were analyzed for the spatial distribution of light intensities as the two fluids mixed. The experimental result showed that complete mixing was achieved in less than 3 min.

II. MATERIALS AND METHODS

A. Design of the reciprocating flow micromixer

The designed system as shown in Fig. 1 consisted of a network of three 240 μm-deep reservoirs R_{U1}, R_{U2}, and R_L, a 60 μm-deep mixing chamber M, and several microchannels of 60×240 μm cross section in a backward J-shaped arrangement. Mixing was investigated by injecting two different sample liquids in reservoirs R_{U1} and R_{U2} located at the top of the "J." The mixing unit was fixed on a rotating holder as shown in Fig. 2(a). The induced centrifugal force drove the two liquids downstream into the common mixing chamber, M, in the middle of the J. With continued rotation, the semimixed fluid continued to flow downstream and into reservoir R_L at the tip of the J, causing compression of the air trapped within that reservoir. The pressure of the compressed air was calculated as:

$$P_{\text{air}} = \left(\frac{V_{R_L}}{V_{R_L V}} - 1 \right) P_{\text{atm}}, \tag{3}$$

where P_{atm} is the atmospheric pressure, V_{R_L} is the volume of the reservoir R_L, and $V_{R_L V}$ is the volume of the vacant section of R_L where the air was pressurized. Since $V_{R_L V}$ decreased as a result of the flow moving into the reservoir R_L, the pressure of the trapped air increased. In order to maintain a constant volumetric flow rate in the mixing chamber, the angular frequency of rotation had to be increased with an experimentally obtained acceleration rate. Once R_{U1} and R_{U2} were emptied, the angular frequency of rotation was gradually reduced, decreasing the centrifugal force, and the compressed air pushed liquid back into M, R_{U1}, and R_{U2}. This cycle of increasing and decreasing angular frequency was repeated two more times, resulting in the complete mixing of the liquids.

B. Fabrication of the SU-8 mold

The mixing microstructure was designed by using SolidWorks 2007 (SolidWorks Corporation, Concord, MA) and fabricated using the soft lithography and rapid prototyping techniques previously reported by Duffy *et al.*[42] Briefly, to fabricate the microchannels and the mixing chamber, a 60 μm thick layer of SU-8 50 negative photoresist (Microchem Inc., Newton, MA) was spun on a 100 cm diameter reclaimed Si wafer (Addison Engineering, San Jose, CA) and baked on a hotplate at 95 °C for 40 min. The wafer was then exposed to ultraviolet light (365 nm) and developed using SU-8 developer (Microchem Inc., Newton, MA). The next step was to spin a thick layer of SU-8 100 on the same platform, followed by repetition of the previous steps in order to create the 240 μm deep reservoirs [Fig. 1(b)]. A MA6 mask aligner (SUSS Micro Tec, Munich, Germany) was used to align the two layers and secure the connection of the channels to the reservoirs.

C. Fabrication and assembly of the mixing unit

A PDMS reactive thermosetting mixture from Dow Coring Corporation, MI, was prepared by mixing the base and the curing agent thoroughly in a weight ratio of 10:1, as per the manufacturer's instructions. After degassing, the PDMS mixture was poured on the SU-8 master mold composed of positive relief structures of channels, reservoirs, and the mixing chamber, followed by curing on a hot plate at 50 °C for 5 h. After curing, the slab of PDMS was peeled off the master, cut to fit within the area of a 25×75 mm glass slide, and punched with inlet holes of 1 mm diameter where appropriate. The slab of PDMS embossed with microfluidic channels and reservoirs was then pressed on the glass slide and bonded overnight in an oven at 70 °C [Fig. 1(c)].

D. Manufacturing of rotor holder

The rotor holder [Fig. 2(a)] was designed as a parametric solid model with SolidWorks 2007. It was then directly digitally manufactured from high strength acrylonitrile butadiene styrene (ABS) material, using the Dimension Elite fused deposition modeling machine (Stratasys Inc., St Paul, MN) running in 0.007 in. resolution mode. After the 3D printing, the rotor was cleaned of the soluble support in an ultrasonic bath at 70 °C for 45 min and dried in an open air at room temperature.

E. Spinstand assembly

The mechanical spinstand used to rotate the rotor was assembled from off-the-shelf components. It consisted of a NEMA 23 servo motor (PMB21B-00114–00) and a driver (PC3406Ai-001-E), both made by Pacific Scientific, Rockfield, IL. The driver was serially connected to a personal computer running the MS Windows XP operating system, using an RS232 cable. The electronic system [Fig. 2(b)] for synchronizing the capture of an image at the correct angular coordinate was achieved by the use of a QRD1114 infrared reflection sensor (OMRON, Tokyo, Japan) detecting a reflective strip on the rotor. The sensor was interfaced with a Schmidt Trigger circuit based on a 74HC14 chip in order to produce square trigger pulses. A SN74LS294 frequency divider chip controlled by an EMANT 300 universal serial bus (USB) card (EMANT Ltd., Singapore), also connected to the personal computer, was used to limit the frequency of pulses going to the laser imaging system to between 8 and 14 Hz. MS Visual Basic 2005 was used to develop the software for control of the spinstand and the frequency divider via the

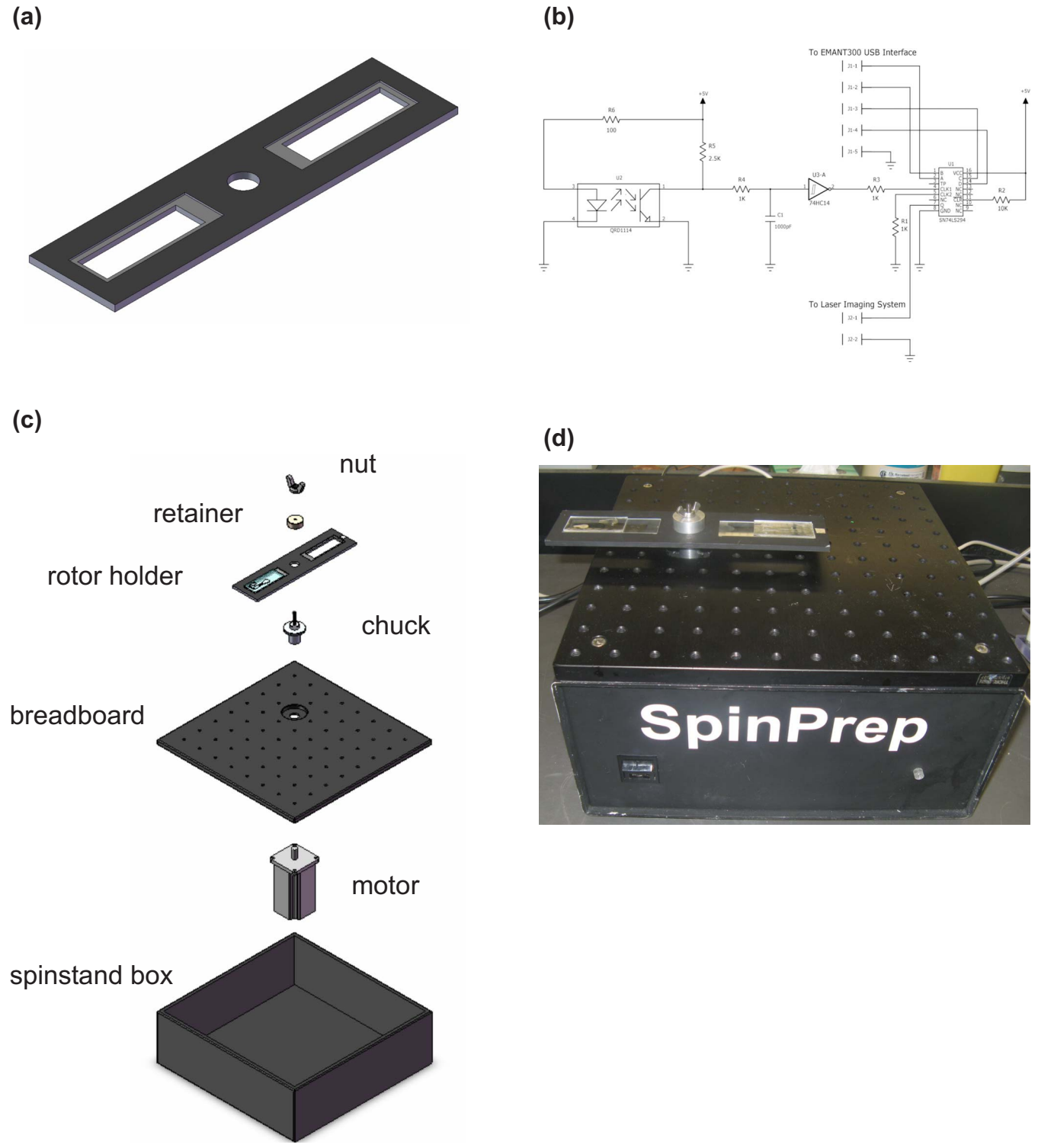

FIG. 2. (Color online) Details of the microfluidics mixer spinstand assembly. (a) 3D solid model and photo of rapid prototyped rotor holder; (b) Schematics of the image acquisition trigger circuit; (c) Exploded view illustration of the spinstand system; (d) Photography of assembled spinstand and rotor holder.

EMANT 300 USB card. Figure 2(c) shows an exploded view of the spinstand solid model while Fig. 2(d) is a photo of the spinstand with a rotor and insert installed.

F. Imaging system setup

The PLIF was used for concentration measurements.[43,44] As deployed, the PLIF system consisted of a high resolution charge coupled device (CCD) camera (PowerView 11MP, 4008×2672 pixels, 12 bit), 400 mJ neodymium doped yttrium aluminum garnet laser (green 532 nm, Blue Sky Research, Milpitas, CA), and a personal computer (PC) workstation (2.66 GHz dual-processor Intel Xeon™). As a fluorescence indicator, an aqueous suspension of fluorescently labeled polystyrene particles was utilized (1% solids by weight, Cat. No #R25, fluorescent polystyrene microsphere suspension, Diagnostics Division, Microgenics Prod-

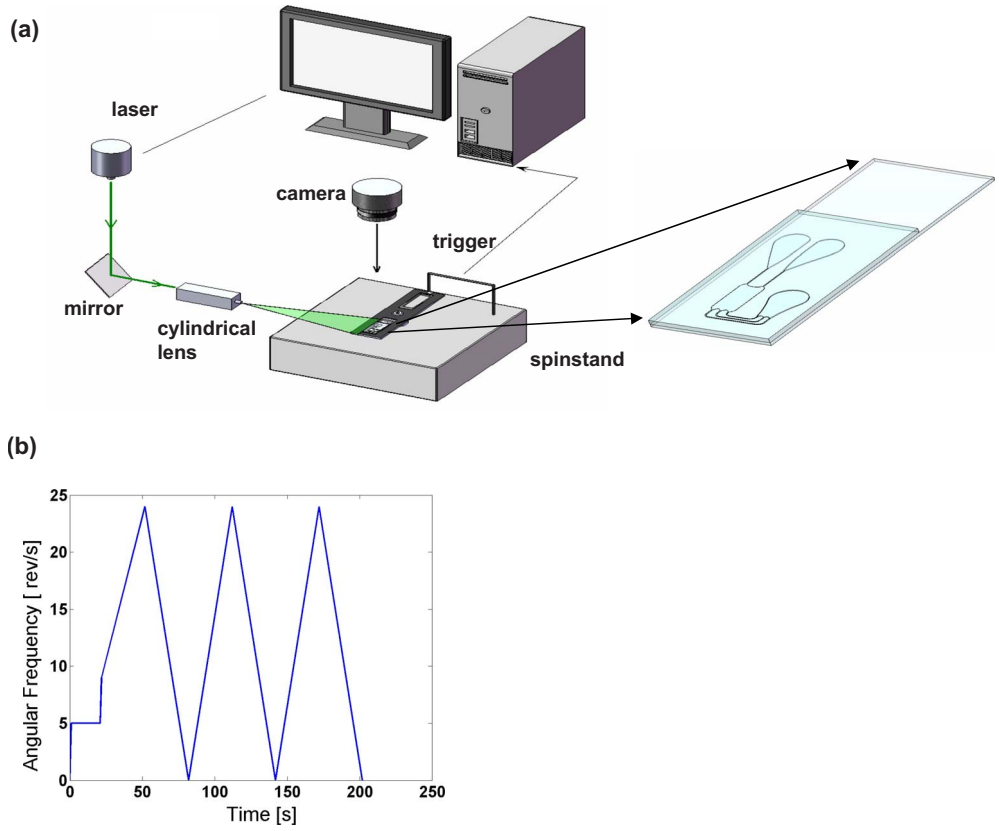

FIG. 3. (Color online) Illustration of the experimental setup: (a) Schematic illustration of the PLIF imaging system; (b) Microfluidics mixer work cycle profile: angular frequency vs time.

ucts from Thermo Fischer Scientific, Freemont, CA). The particles contain embedded fluorescence dye within the polystyrene matrix, with an excitation maximum at 542 nm and an emission maximum at 612 nm, with a refractive index of 1.59 and a suspension density of 1.06 g/cm^3. The suspension of particles was injected into the first reservoir. The second reservoir was filled with distilled water, which does not exhibit fluorescence. A synchronizer (610035, TSI Inc., Shoreview, MN) was utilized to trigger the laser pulse and the camera with correct sequences and timing. A cylindrical lens (−15 mm focal length) was mounted at the end of the laser arm to form a laser light sheet from a laser beam. A Nikon lens (50 mm, $f/1.8$) was used at the camera with a red pass filter (545AGLP-RED 36297). The exposure time was 410 μs and the aperture was set to 5.6. The Q-switch was set to 100 μs corresponding to approximately 50% of the maximum laser power. A schematic view of the imaging system is displayed in Fig. 3(a). A total of 600 images were taken to capture three cycles of mixing. Each image covered an area of 50×60 mm stored in 30 000 data points each corresponding to a block of 8×8 pixels. All images (tiff) were preprocessed into ASCII files using INSIGHT 3G (TSI, Inc., Shoreview, MN) and further processed using custom made MATLAB routines.

G. Experimental procedure

In order to examine changes in concentration gradients in the mixer, 8 μl of purified de-ionized (DI) water and 8 μl of a suspension of red fluorescing polymer microspheres were injected into the top reservoirs R_{U1} and R_{U2}, respectively. The loaded PDMS/glass unit was placed on the rectangular platform and immediately mounted onto the spinstand to avoid sample evaporation. The spin program was set according to the angular frequency profile presented in Fig. 3(b). The alignment of the laser was performed at a low angular frequency (5 s^{-1}) with the spinning time of 20 s. After the alignment was established, the angular frequency was increased up to the "burst frequency,"[39] which is the frequency at which the centrifugal force intensity overcomes the capillary force, advancing the liquid into the microchannels. For our device, the burst frequency was calculated and experimentally verified as 10 s^{-1}. Immediately after the burst frequency was reached, the spin speed was further increased to 24 s^{-1} for the next 30 s in order to build up the pneumatic pressure in R_L, and to maintain an average flow rate of 10 μl/min. At the end of this stage the upper reservoirs R_{U1} and R_{U2} were fully emptied. In order to reverse the direction of the flow and thus allow chaotic mixing, angular frequency was decreased to zero in the next 30 s. At the end of this half cycle the lower reservoir, R_L, was completely empty of fluid. The optimal angular velocities and the timing were experimentally determined using the same sample fluids. A sequence of PLIF images taken during the mixing procedure are presented in Figs. 4(a)–4(e). Images were calibrated to eliminate the false intensity effects due to the proximity of the camera to the mixing chamber M and laser light reflections. To calibrate the light intensity to concentration, equal parts of fluorescent particles and DI water were mixed thoroughly and injected into inlet holes at R_{U1} and R_{U2} and a still image of the mixing chamber was taken after spinning

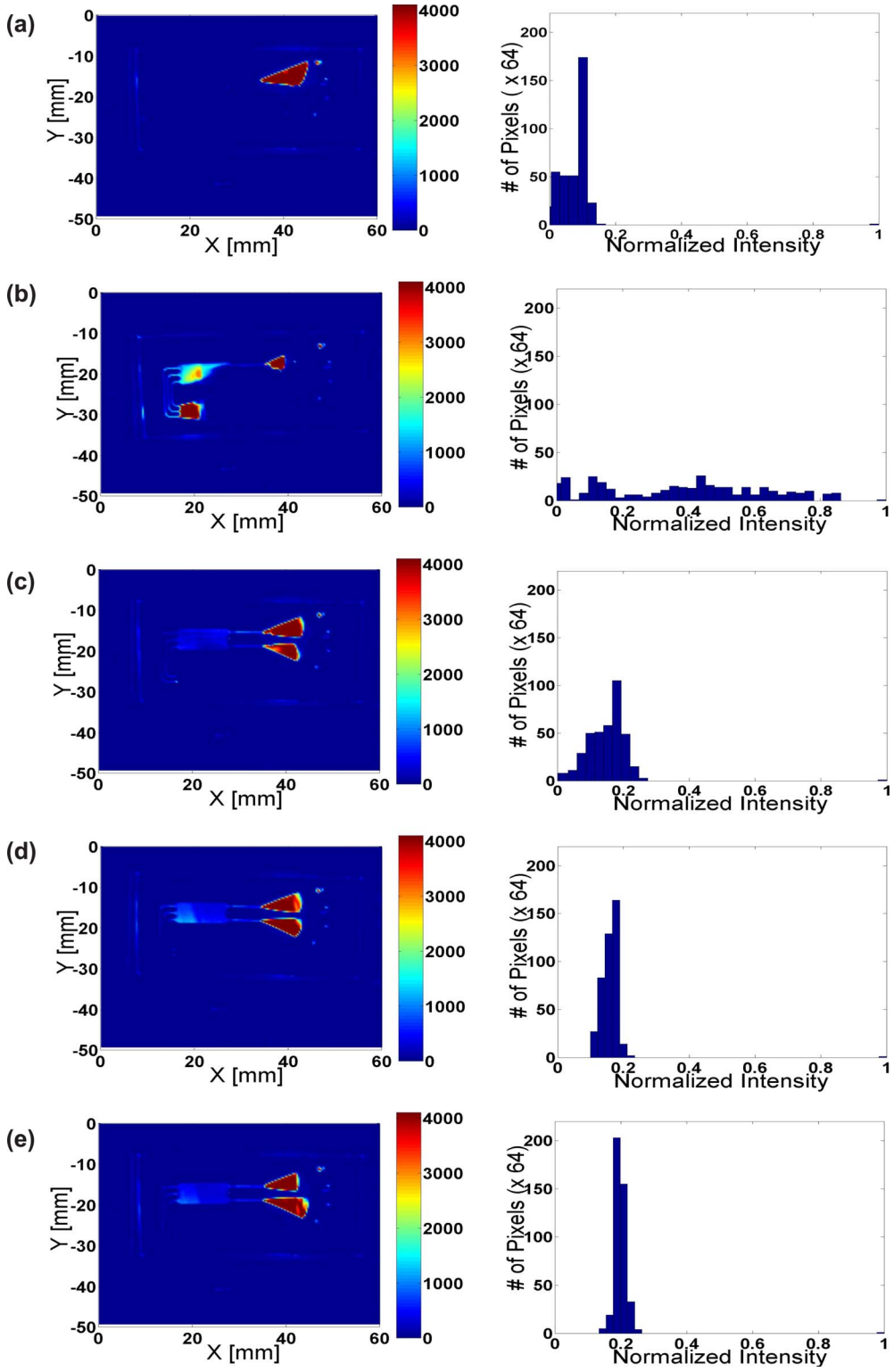

FIG. 4. (Color online) Selected sequential planar laser induced fluorescence intensity maps obtained from processed video frames during different stages of mixing and corresponding histograms (a: at time 0 s; b: at time 30 s; c: at time 60 s; d: at time 120 s; e: at time 180 s).

the system for one cycle. For each (i,j) position in the mixing chamber, calibration was performed according to the following equation:

$$I_{i,j,C} = I_{i,j} - \left(Ic_{i,j} - I_{\mathrm{MAX}} \frac{D_R}{D_M} \right), \tag{4}$$

where $I_{i,j,C}$ was the corrected intensity, $I_{i,j}$ was the measured intensity, $Ic_{i,j}$ was the intensity collected from the calibration image, I_{MAX} was the maximum possible intensity of 4096, D_R was the depth of reservoirs (240 μm), and D_M was the depth of the mixing chamber (60 μm).

III. RESULTS AND DISCUSSION

One of the common ways to estimate the mixing efficiency is to utilize the distribution of the intensity of a fluo-

rescently labeled compound over the mixing area. This can be done either by labeling only one of the two mixing compounds or by using two labels with different colors for both mixing compounds. In this particular case, we decided to label fluid in only one of the chambers. In such arrangement, progression of the mixing process is observed by following spatial and/or temporal variation in fluorescence intensity of the mixture over the defined mixing volume or path. The quantifying factor of mixing efficiency will be a standard deviation of the fluorescence intensity in any particular spot versus the entire studied area or path. Such standard deviation is commonly referred as a mixing index.[13,31,44] Standard deviation or mixing index, as herein defined, is the deviation of the light intensity in the mixing chamber from the mean value of the intensity over its entire area. A lower value of the standard deviation indicates a more homogenous mixture and a higher mixing efficiency. A zero valued standard deviation corresponds to a fully mixed chamber in an ideal situation. However, even in the case of a theoretically perfect mixing device, any practical measurement will show a nonzero standard deviation observed due to systemic error/fluctuation of pixel intensities of the imaging system.

The Figs. 4(a)–4(e) represent histograms of the values of normalized fluorescence intensity as measured over the entire mixing chamber. In the case of our mixer, mixing caused the fluorescence intensity to become more uniformly distributed, resulting in an increasingly narrower peak centered at normalized value of 0.2. Figure 5(a) represents the progression of the mixing index based on the standard deviation versus the cycle number with cycle zero corresponding to $t=0$ s. We observe a progressive decrease in the standard deviation with each cycle, indicating an increase in fluid mixing with time. Based on the obtained results, it can be concluded that complete mixing of the two fluids is achieved after three complete cycles of flow oscillation.

We hypothesize that fluid mixing in this device is due to the interplay of two different phenomena. First, as seen in Fig. 4(b), at time $t=30$ s at the end of the first half cycle, the fluorescent particles are deviating from the radial direction as the micromixer spins. This is due to the effect of the Coriolis force that bends the flow in the negative x direction as it moves downstream in the mixing chamber. In this experimental setup, the holder rotated in a clockwise direction similar to that in Fig. 5(b), and therefore the Coriolis force acted in the direction shown in the figure, shifting the fluorescent particles opposite to the direction of rotation. As the fluid reversed its direction, the pneumatic pressure forces the two adjacent fluids to mix. Second, observations herein presented suggest that mixing is partially achieved in the mixing chamber due to the flexible nature of PDMS. When the holder was rotated, the mixing chamber deformed by expanding vertically and some of the fluid appeared to travel to the center of the chamber to fill up the area. This effect was verified by measuring the total occupied volume (including the volumes of the microchannels, mixing chamber, and the occupied section of R_L) at the end of a half cycle when the angular frequency of rotation was at its peak with the assumption that the PDMS did not deform, and comparing this volume with the volume of the liquid that was initially injected in the inlet holes. The difference in these two values (~ 5 μl) represents the amount of fluid that occupied the deformed section of the mixing chamber, M, and the lower reservoir R_L. The deformation or bellowing effect can also be viewed in the image taken at time $t=30$ s in Fig. 4(a) where the color of the fluorescent particles is more intense in the middle of the chamber than closer to the walls. When the angular frequency of rotation was reduced, the chamber contracted and pushed liquid back toward the edges of the chamber. This probably contributed to the mixing.

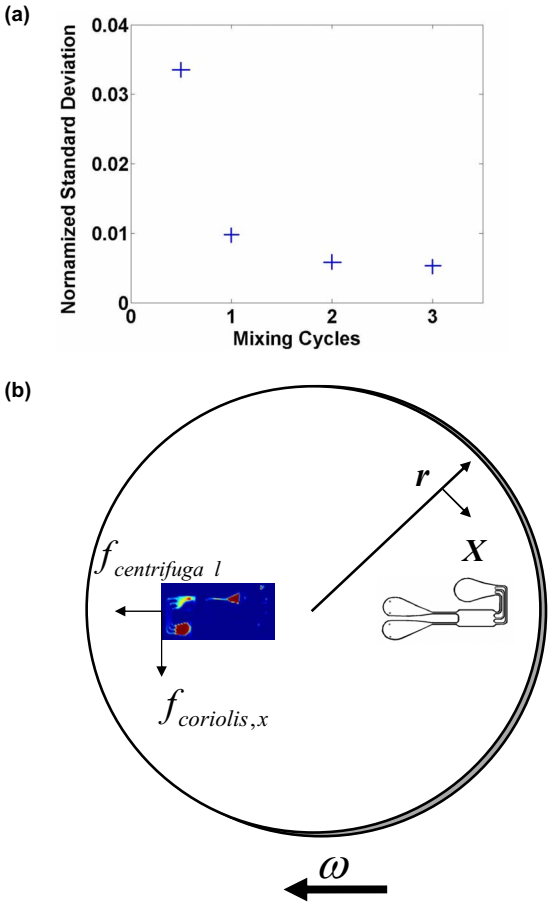

FIG. 5. (Color online) (a) Progression of the standard deviation of the pixel intensity; (b) Schematic of the forces acting on the fluid elements in the mixer.

IV. CONCLUSIONS

We presented an elegant new way for microfluidic mixing on a centrifugal platform by inducing local chaotic advection in the fluid flow by use of the Coriolis force, the centrifugal force, reciprocating flow, and oscillatory volume contractions. As such it is ideally suited for use for reagents mixing on the centrifugal microfluidic total analysis system such as compact disk-like or rotating cartridge analytical and *in vitro* diagnostics platforms. The major benefits of this novel device are its simplicity, robustness, and low cost of manufacturing. Those benefits come from the fact that the presented device does not require any separate active components like pumps, active valves, physical passive energy or flow directing structures, and that it is entirely operated only by changing the angular frequency of the rotor. In this case,

simply by programming the temporal trajectory of the spinning disk or cartridge, a reciprocal motion of the liquid was induced, which created efficient mixing by induction of local chaotic flow at a low Re number. The proposed system could be easily integrated into any existing centrifugal microfluidic-based device, with a minimum consumption of disk or cartridge space, and minimal modifications. This is especially useful for molecular biology and molecular diagnostics types of applications, and other applications that may be sensitive to the shear force destruction of macromolecules such as nucleic acid analysis. The absence of separate mechanical applicators or energy directors decreases the possibility of shearing of nucleic acids during the mixing process.

ACKNOWLEDGMENTS

This research was supported by the National Science Foundation's Graduate Research Fellowship, Grant No. DGE-0808392. We would like to thank Mr. Jeffrey Whyte from MP Biomedicals LLC, Santa Ana, California for his assistance with rapid prototyping of the rotor and Mr. Vu Phan from the INRF clean room facility at UC Irvine for his help with fabrication of the SU-8 molds.

[1] S. Haeberle and R. Zengerle, Lab Chip **7**, 1094 (2007).
[2] M. A. McClain, C. T. Culbertson, S. C. Jacobson, N. L. Allbritton, C. E. Sims, and J. M. Ramsey, Anal. Chem. **75**, 5646 (2003).
[3] A. J. de Mello, Nature (London) **442**, 394 (2006).
[4] D. Sparks, R. Smith, M. Straayer, J. Cripe, R. Schneider, A. Chimbayo, S. Anasari, and N. Najafi, Lab Chip **3**, 19 (2003).
[5] A. Daridon, M. Sequeira, G. Pennarun-Thomas, H. Dirac, J. P. Krog, P. Gravesen, J. Lichtenberg, D. Diamond, E. Verpoorte, and N. F. de Rooij, Sens. Actuators B **76**, 235 (2001).
[6] K. M. Horsman, J. M. Bienvenue, K. R. Blasier, and J. P. Landers, J. Forensic Sci. **52**, 784 (2007).
[7] B. M. Paegel, R. G. Blazej, and R. A. Mathies, Curr. Opin. Biotechnol. **14**, 42 (2003).
[8] T. H. Schulte, R. L. Bardell, and B. H. Weigl, Clin. Chim. Acta **321**, 1 (2002).
[9] D. Beebe, M. Wheeler, H. Zeringue, E. Walters, and S. Raty, Theriogenology **57**, 125 (2002).
[10] Y. C. Tan, K. Hettiarachchi, M. Siu, and Y. P. Pan, J. Am. Chem. Soc. **128**, 5656 (2006).
[11] M. J. Madou, *Fundamentals of Microfabrication, Science of Miniaturization*, 2nd ed. (CRC, Boca Raton, 2002).
[12] H. A. Stone, A. D. Stroock, and A. Ajdari, Annu. Rev. Fluid Mech. **36**, 381 (2004).
[13] K. S. Ryu, K. Shaikh, E. Goluch, Z. F. Fan, and C. Liu, Lab Chip **4**, 608 (2004).
[14] B. R. Munson, D. F. Young, and T. H. Okiishi, *Fundamentals of Fluid Mechanics*, 5th ed. (Wiley, New York, 2006).
[15] F. P. Incropera, D. P. DeWitt, T. L. Bergman, and A. S. Lavine, *Fundamentals of Heat and Mass Transfer*, 6th ed. (Wiley, New York, 2007).
[16] J. M. Ottino and S. Wiggins, Philos. Trans. R. Soc. London, Ser. A **362**, 923 (2004).
[17] M. A. Stremler, F. R. Haselton, and H. Aref, Philos. Trans. R. Soc. London, Ser. A **362**, 1019 (2004).
[18] M. J. Madou, *Fundamentals of Microfabrication and Nanotechnology*, 3rd ed. (CRC, Boca Raton, 2009).
[19] I. Glasgow, J. Batton, and N. Aubry, Lab Chip **4**, 558 (2004).
[20] L.–H. Lu, K. S. Ryu, and C. Liu, J. Microelectromech. Syst. **11**, 462 (2002).
[21] H. Kido, M. Micic, D. Smith, J. Zoval, J. Norton, and M. J. Madou, Colloids Surf., B **58**, 44 (2007).
[22] I. Glasgow and N. Aubry, Lab Chip **3**, 114 (2003).
[23] Z. Yang, H. Goto, M. Matsumoto, and R. Maeda, Electrophoresis **21**, 116 (2000).
[24] P. Garstecki, M. J. Fuerstman, M. A. Fischbach, S. K. Sia, and G. M. Whitesides, Lab Chip **6**, 207 (2006).
[25] X. Casadevall i Solvas, R. A. Lambert, L. Kulinsky, R. H. Rangel, and M. J. Madou, Micro and Nanosyst. **1**, 2 (2009).
[26] V. Hessel, H. Lowe, and F. Schonfeld, Chem. Eng. Sci. **60**, 2479 (2005).
[27] Y. C. Chung, Y. L. Hsu, C. P. Jen, M. C. Lu, and Y. C. Lin, Lab Chip **4**, 70 (2004).
[28] F. G. Bessoth, A. J. de Mello, and A. Manz, Anal. Commun. **36**, 213 (1999).
[29] J. Branebjerg, P. Gravesen, J. P. Krog, and C. R. Nielsen, Proceedings of IEEE-MEMS '96, San Diego, CA, 12–15 February 1996 (unpublished), p. 441.
[30] D. S. Kim, S. H. Lee, T. H. Kwon, and C. H. Ahn, Lab Chip **5**, 739 (2005).
[31] R. H. Liu, M. A. Stremler, K. V. Sharp, M. G. Olsen, J. G. Santiago, R. J. Adrian, H. Aref, and D. J. Beebe, J. Microelectromech. Syst. **9**, 190 (2000).
[32] C. C. Hong, J. W. Choi, and C. H. Ahn, Lab Chip **4**, 109 (2004).
[33] F. Schonfeld, V. Hessel, and C. Hofmann, Lab Chip **4**, 65 (2004).
[34] C. Neils, Z. Tyree, B. Finlayson, and A. Folch, Lab Chip **4**, 342 (2004).
[35] C. Simonnet and A. Groisman, Phys. Rev. Lett. **94**, 134501 (2005).
[36] V. Hessel, S. Hardt, H. Lowe, and F. Schonfeld, AIChE J. **49**, 566 (2003).
[37] S. H. Wong, M. C. L. Ward, and C. W. Wharton, Sens. Actuators B **100**, 359 (2004).
[38] P. Tabeling, M. Chabert, A. Dodge, C. Jullien, and F. Okkels, Philos. Trans. R. Soc. London, Ser. A **362**, 987 (2004).
[39] D. Gobby, P. Angeli, and A. Gavriilidis, J. Micromech. Microeng. **11**, 126 (2001).
[40] S. I. Masca, and I. R. Rodriguez-Mendieta, Rev. Sci. Instrum. **77**, 055105 (2006).
[41] S. Lai, S. N. Wang, J. Luo, L. J. Lee, S. T. Yang, and M. J. Madou, Anal. Chem. **76**, 1832 (2004).
[42] D. C. Duffy, J. C. McDonald, O. J. A. Schueller, and G. M. Whitesides, Anal. Chem. **70**, 4974 (1998).
[43] J. P. Crimaldi, Exp. Fluids **44**, 851 (2008).
[44] P. E. Arratia and F. J. Muzzio, Ind. Eng. Chem. Res. **43**, 6557 (2004).